Nanoscale

Degradable polyphosphoester–based silver–loaded nanoparticles as therapeutics for bacterial lung infections

Nanoscale

COMMUNICATION

Degradable polyphosphoester-based silver-loaded nanoparticles as therapeutics for bacterial lung infections

Fuwu Zhang,[a] Justin A. Smolen,[b] Shiyi Zhang,[a] Richen Li,[a] Parth N. Shah,[b] Sangho Cho,[a] Hai Wang,[a] Jeffery E. Raymond,[a] Carolyn L. Cannon*[b] and Karen L. Wooley*[a]

In this study, a new type of degradable polyphosphoester-based polymeric nanoparticle, capable of carrying silver cations *via* interactions with alkyne groups, has been developed as a potentially effective and safe treatment for lung infections. It was found that up to 15% (w/w) silver loading into the nanoparticles could be achieved, consuming most of the pendant alkyne groups along the backbone, as revealed by Raman spectroscopy. The well-defined Ag-loaded nanoparticles released silver in a controlled and sustained manner over 5 days, and displayed enhanced *in vitro* antibacterial activities against cystic fibrosis-associated pathogens and decreased cytotoxicity to human bronchial epithelial cells, in comparison to silver acetate.

Despite current advancements in modern medicine, infectious diseases, especially pulmonary infections, continue to pose great clinical challenges to successful medical treatment.[1, 2] In 2012, lower respiratory infections were reported as the second leading cause of years-of-life lost (YLL) worldwide.[3] One of the contributing factors is widespread antibiotic resistance, which enables antibiotic-resistant bacteria, such as *Enterococcus faecium, Staphylococcus aureus, Klebsiella pneumoniae, Acinetobacter baumanii, Pseudomonas aeruginosa,* and *Enterobacter species* (ESKAPE), to survive despite treatment with existing antibacterial drugs.[2, 4, 5] The growing number of multi-drug resistant strains has made imperative the development of new antibiotics and novel approaches to deliver existing agents.[2, 6-8]

Silver has been used as an antimicrobial agent for centuries, especially in the topical treatment of wounds and burns.[9] Silver cations are well known to be highly toxic against a broad spectrum of microorganisms, while metallic silver has minimal antimicrobial activity.[10-12] Although their biocidal mechanisms are not fully understood, silver cations have been reported to cause bacterial protein denaturation, enzyme oxidation, and interference with DNA replication.[13, 14] Furthermore, unlike traditional antibiotics, silver cations exhibit low toxicity to human tissues and documented instances of bacterial resistance are rare.[1, 15, 16] Therefore, various silver-based antimicrobials have been developed. For example, silver sulfadiazine (AgSD) cream, which was introduced in the 1960s, has become a routine remedy in the treatment of burns over the last few decades.[9, 17] However, silver cation-based small molecules are often not practical *in vivo*, because free Ag^+ will interact with anions and other biological compounds in the human body, decreasing the bioavailability of free Ag^+.[1, 12, 18] Therefore, there is a remaining need to develop a drug-delivery system that can effectively carry the silver-based antimicrobials to the infected tissues with minimal inactivation of these drugs.

Recently, several nanosized systems for the delivery of silver-based small molecules have been developed to improve bioavailability and efficacy.[18-22] Our group has investigated shell crosslinked knedel-like (SCK) nanoparticles, comprised of poly(acrylic acid)-*block*-polystyrene (PAA-*b*-PS) block copolymers, for the packaging and delivery of both silver cation and hydrophobic 1-hexyl-3-methyl-4,5-dichloro-imidazole-2-ylidene silver(I) acetate (silver carbene complex, SCC10). Although these PAA-*b*-PS based SCKs displayed lower antimicrobial activities compared to $AgNO_3$ *in vitro*, they exhibited remarkably-enhanced therapeutic efficacy *in vivo*.[20, 21] A key drawback to these materials, however, is their stable, non-degradable structure, which raises concerns about their clearance from the body, possible side effects from their extended retention, and also their environmental persistence. Moreover, the electrostatic interaction between silver cations and the carboxylates of the acrylic acid residues is weak, leading to instability, formation of AgCl precipitates when challenged by saline solution, and relative ineffectiveness *in vivo* for the SCKs loaded only with Ag cations.[20, 21]
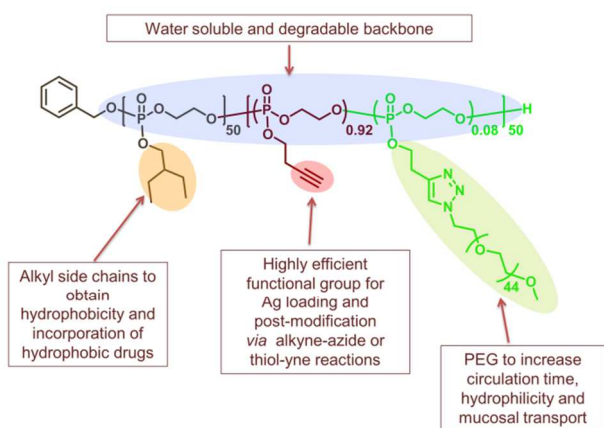
Fig. 1 Overall design of the degradable amphiphilic block terpolymer for assembly into nanoparticles capable of silver-based antimicrobial delivery.

To address these problems, we have designed and synthesized an amphiphilic block terpolymer with a hydrolytically-degradable polyphosphoester-based backbone and side chain functionalities that allow for stronger binding of silver cations (Fig. 1).[23-27] The alkyne side chains are designed to incorporate silver *via* reversible interactions between silver cations and alkynes, which has been traditionally employed in various catalytic processes.[28-31] A portion of the alkynes was consumed for the installation of methoxypolyethylene glycol (mPEG), which was grafted onto the backbone *via* copper(I)-catalyzed alkyne-azide cycloaddition (CuAAC) reactions to increase hydrophilicity and enhance mucosal transport.[32-36] These alkyne groups also offer opportunities for further modifications, such as crosslinking to increase nanoparticle stability and addition of fluorescent probes or radiolabeling sites for investigation of trafficking *in vitro* and *in vivo*.[24, 33, 37-39] Finally, the alkyl side chains impart hydrophobicity, allowing the formation of micelles with core-shell morphology, as well as providing avenues to load potential hydrophobic drugs, for example hydrophobic silver carbene complexes including SCC10,[19] for combination drug delivery.

The amphiphilic block terpolymer PEBP-*b*-PBYP-*g*-PEG was synthesized by utilizing click-type chemistries (Scheme 1).[23] Hydrophobic-functional AB diblock polyphosphoesters PEBP-*b*-PBYP were synthesized by one-pot sequential ring-opening polymerizations (ROP) of hydrophobic monomer 2-ethylbutoxy phospholane (EBP) and alkyne-functionalized 2-butynyl phospholane (BYP) in dichloromethane, with benzyl alcohol as the initiator. PEGylation was achieved *via* CuAAC of PEBP-*b*-PBYP by reaction with azido-terminated mPEG of 2 kDa molecular weight in *N,N*-dimethylformamide (DMF), followed by purification using Sephadex G-25 size exclusion chromatography and extensive dialysis against nanopure water to remove copper and other impurities. The gel permeation chromatographic (GPC) analysis (Fig. 2) demonstrated the
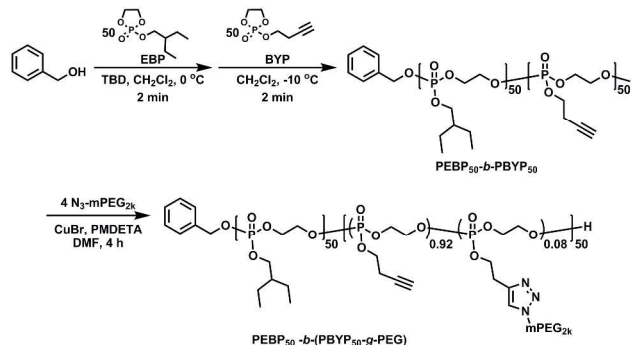
Scheme 1 Synthesis of PEBP-*b*-PBYP-*g*-PEG *via* sequential ring-opening polymerizations of EBP and BYP, followed by PEGylation *via* CuAAC.
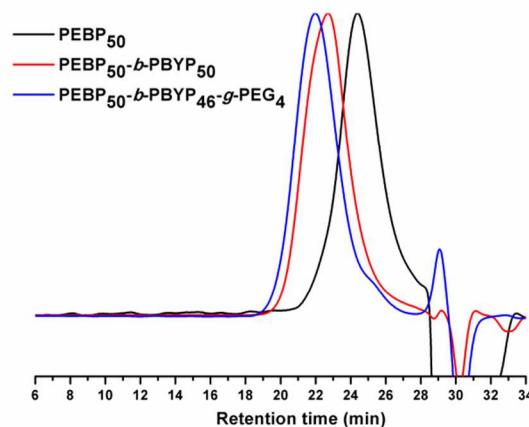

Fig. 2 GPC traces of PEBP homopolymer (black line, PDI = 1.20), PEBP-*b*-PBYP diblock copolymer (red line, PDI = 1.25) and PEBP-*b*-PBYP-*g*-PEG terpolymer (blue line, PDI = 1.26).

successful chain extension from homopolymer PEBP, with a peak maximum retention time at 24.5 min, to obtain the diblock copolymer PEBP-*b*-PBYP, having a peak maximum at 22.7 min. GPC also allowed for confirmation of grafting by PEG, with an observed >98% reduction in the intensity of the non-grafted PEG signal (25.6 min) and a shift of the grafted polymer product to shorter retention time (22.0 min) (Fig. 2).

Due to the water-soluble polyphosphoester backbone and densely-grafted mPEG, the amphiphilic block terpolymers could be directly dissolved in nanopure water at concentrations up to 120 mg/mL after 5 min sonication, during which they spontaneously formed micellar nanoparticles (Fig. 3). These micelles were found to have a number-averaged hydrodynamic diameter of 11 ± 3 nm with monomodal size distribution and a low polymer dispersity of 0.25, as measured by dynamic light scattering (DLS) (Fig. 4a). The circular images observed by transmission electron microscopy (TEM) suggested that these nanoparticles were spherical with uniform sizes of 35 ± 4 nm (Fig. 4c). The significantly greater diameter by TEM *vs*. DLS also suggested that the particles deformed and flattened to a
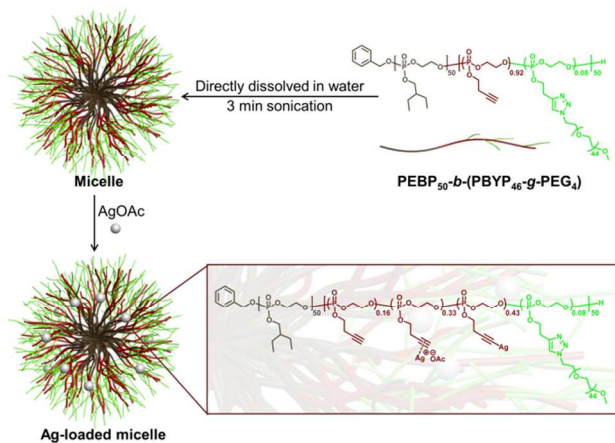
Fig. 3 Schematic representation of micelle construction *via* self-assembly of the amphiphilic terpolymers in water, followed by loading with silver acetate (AgOAc).

great extent upon deposition from solution and drying onto the carbon-coated copper grids for TEM imaging. Atomic force microscopy (AFM) was, therefore, conducted, and found to give an average height value measured as 0.82 nm, confirming that deformation occurred upon deposition onto a mica substrate (Fig. S2 a&b). The flattening phenomenon observed by TEM and AFM could be attributed to the intrinsic low glass transition temperature (-52 ºC) of the polyphosphoester backbone.

Silver loading was subsequently performed after successful micellization, using silver acetate as the Ag^+ source to avoid potential inflammatory response from $AgNO_3$, which was used in the previous study (Fig. 3).[20] The reaction mixture of micelles and silver acetate was stirred overnight to ensure maximum loading efficiency, followed by purification by passing through centrifugal filter devices (MWCO 100 kDa) several times (N>3) to remove unreacted silver acetate. The actual loading was measured by inductively coupled plasma mass spectrometry (ICP-MS), using Rh as an internal standard. Different Ag feeding ratios were tested to optimize conditions with appropriate loading efficiency and loading amount (Fig. S1). At feeding ratios below 1 (Ag^+:alkyne), the loading amount increased approximately linearly, with only a slight
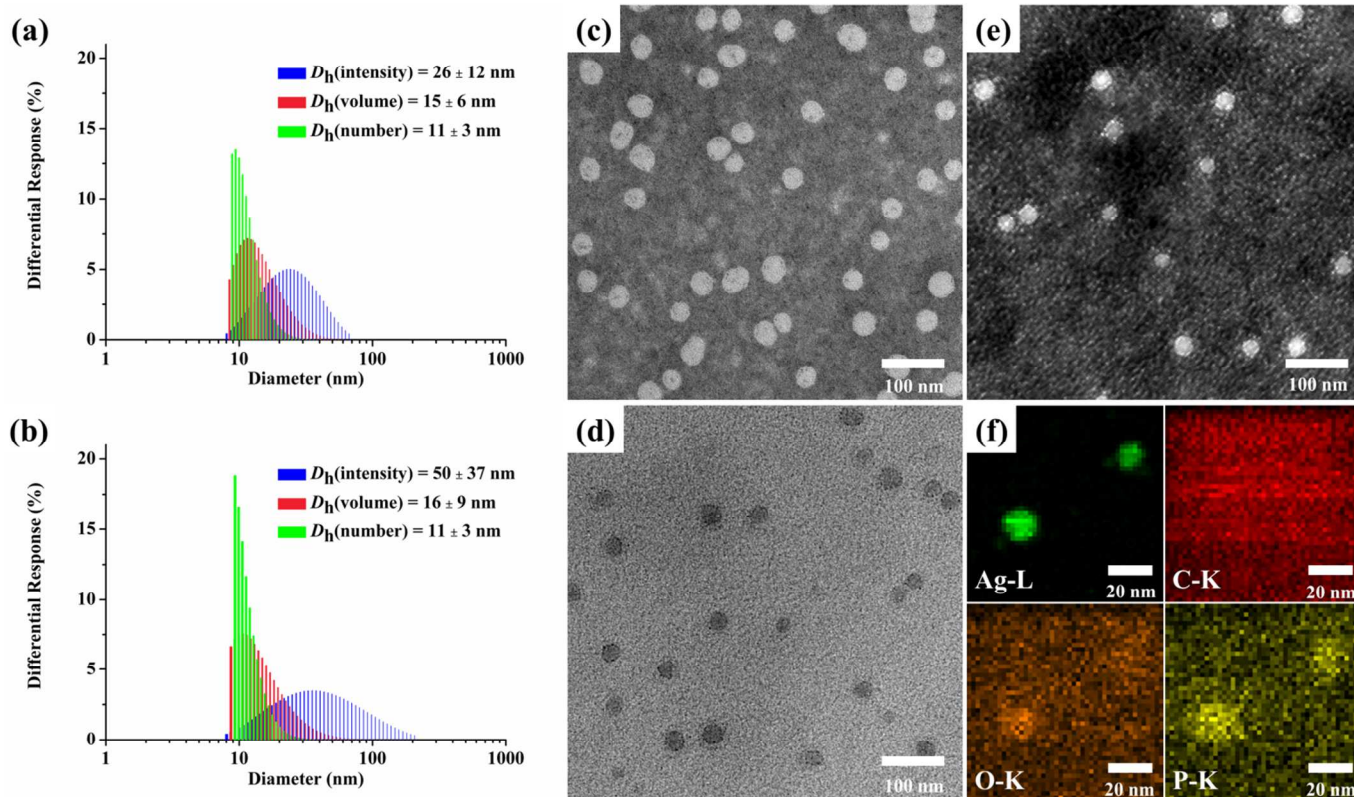
Fig. 4 Characterization of nanoparticles. DLS histograms of intensity-averaged (D_h(intensity)), volume-averaged (D_h(volume)), number-averaged (D_h(number)) hydrodynamic diameters of (a) micelles, and (b) Ag-loaded micelles. Bright-field TEM images of (c) micelles, stained by uranyl acetate, and (d) Ag-loaded micelles. Dark-field STEM image (e), and elemental mapping (f) of Ag-loaded micelles. The silver-loaded micelles were not stained in all samples.

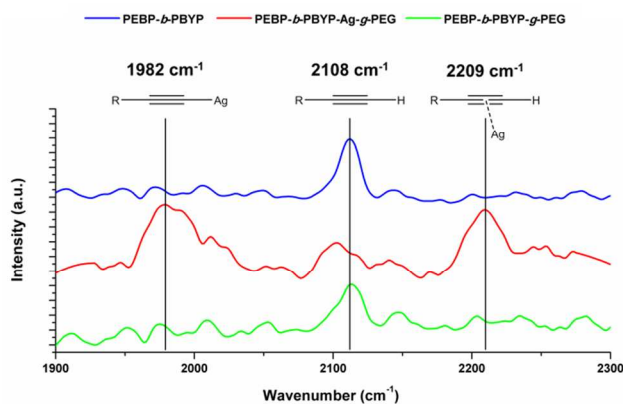**Fig. 5** Raman spectroscopy of PEBP-*b*-PBYP (blue line), PEBP-*b*-PBYP-*g*-PEG (green line), and Ag-loaded micelles (PEBP-*b*-PBYP-Ag-*g*-PEG, feeding ratio = 1, red line).

drop in the loading efficiency, indicating reliability of the chemistry. A higher amount of silver loading was achieved with a maximum 15% loading (w/w), though much lower loading efficiency was observed as the feeding ratio continued to rise above 1. The feeding ratio of 1 was chosen for further characterization and biological evaluation, as it provided a good balance between loading amount and efficiency.

The sizes and size distributions of these Ag-loaded micelles were also characterized by DLS and TEM. These data suggest that silver loading had minimal effect on the number-averaged hydrodynamic diameter of the micelles, with an average diameter remaining at *ca.* 11 nm. No staining of the Ag-loaded micelles is needed, since Ag is of high atomic number, which provides sufficient image contrast. Both bright-field TEM and high-angle annular dark-field imaging in the scanning TEM mode (HAADF-STEM) confirmed that well-defined silver-loaded nanoparticles were prepared, with relatively uniform dry-state substrate-adsorbed diameters of *ca.* 30 nm (Fig. 4d&e). As observed for the non-loaded micelles, comparisons of TEM and AFM images indicated that these silver-loaded nanoparticles underwent severe deformation upon deposition and drying, giving AFM-measured height and diameter values of *ca.* 1.0 nm and *ca.* 30 nm, respectively, on a mica substrate (Fig. S2 c&d). Elemental mapping was performed on the Ag-loaded nanoparticles using an energy-dispersive X-ray spectroscopy (EDS) detector in the STEM mode. The co-localization of silver, oxygen and phosphorous further demonstrated that silver was loaded into the polymeric matrix (Fig. 4f).

The 1:1 silver-incubated sample was assessed by Raman spectroscopy to determine the extent and nature of silver-yne interactions (Fig. 5). Both the block copolymer PEBP-*b*-PBYP and block terpolymer PEBP-*b*-PBYP-*g*-PEG displayed only one peak in the region of 1900-2300 cm^{-1}, corresponding to the

terminal alkyne groups present as side chain functionalities along one block of the polymer backbone.[30] In the case of silver-loaded nanoparticles, two additional peaks at 1982 and 2209 cm^{-1} were observed and were assigned to silver acetylide and Ag-alkyne complex, respectively.[30, 40, 41] An integrated signal intensity assessment of the number of subunits in each state, presuming comparable scattering cross-sections for each species, was performed, and revealed that *ca.* half of the alkyne functionalities were covalently bound to silver, with a third π-associated to silver, and that the remainder did not react.

Release of silver from the nanoparticles was evaluated by monitoring the decrease of silver concentration inside dialysis cassettes at 37 ºC, analysed by ICP-MS (Fig. 6). It was found that silver was released in a sustained and controlled manner in nanopure water, with a release half-life $t_{1/2}$ of 28 h. The release was also conducted in 10 mM phosphate buffer containing 10 mM NaCl, to mimic the *in vivo* environment in patients with lung infection. As expected, the presence of NaCl significantly accelerated silver release due to the formation of AgCl, where the $t_{1/2}$ decreased from 28 h to 16 h. The sustained and controlled release of therapeutics may improve efficacy and reduce side effects. In addition, slow release kinetics allow a lower dosing frequency, which offers convenience to enhance patient adherence, as well as potential cost reduction. Furthermore, the silver-loaded nanoparticles were stable in PBS for more than 2 days without visible precipitation, thus displaying the superior stability needed for *in vitro* and *in vivo* applications.
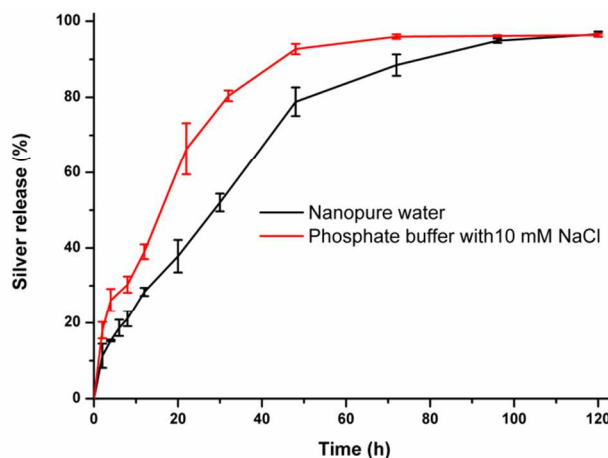

Fig. 6 Release of Ag that was loaded into micelles at 37 ºC in nanopure water (black line) and 10 mM phosphate buffer with 10 mM NaCl, as measured by ICP-MS of aliquots collected from the cassettes over five days.

The antimicrobial potency of the silver-loaded nanoparticles was examined by broth micro dilution to determine the minimum inhibitory concentrations (MICs) and minimum bactericidal concentrations (MBCs) against cystic fibrosis-

associated pathogens *Pseudomonas aeruginosa*, *Staphylococcus aureus*, and *Burkholderia sp.* (Table 1). Strains tested included a laboratory strain of *P. aeruginosa* (PAO1), USA300 *S. aureus* (TCH1516), and strains isolated from cystic fibrosis patients (PAM57-15, PAHP3, SALL06, SAEH05, BG80, and BM54). The MICs and MBCs of the silver nanoparticles were compared with silver acetate and generally showed enhanced antimicrobial potency against these pathogens, with a reduction of MICs by 50% and similar MBCs. *P. aeruginosa* and *Burkholderia sp.* were more susceptible to silver than *S. aureus*, which was resistant to complete killing by silver in the case of TCH1516 and SALL06. The silver-loaded nanoparticles did show a remarkably higher potency against *S. aureus* strain SAEH05, which was not resistant to killing by silver. The increased antibacterial activities of silver-loaded nanoparticles over silver acetate might be ascribed to their increased stability in the aqueous environment and possibly superior association and/or uptake by the bacteria.[42] Furthermore, the silver-loaded nanoparticles displayed decreased toxicity compared with silver acetate, towards a cell line derived from human bronchial epithelial cells (16HBE), though it was not significantly different, as determined by nonparametric Student's t-test (Fig. S3). The increased antibacterial activities and decreased cytotoxicities towards human healthy cells demonstrated the advantages of using nanosized delivery systems for silver-based therapeutics *in vitro*, and suggest their great potential *in vivo*.

Table 1 MICs and MBCs of silver acetate and the silver-loaded micelles against cystic fibrosis pathogens. The MIC/MBCs were performed three times and the values reported represent the highest MIC/MBCs amongst the replicates. Concentration of silver-loaded micelles based on mass of silver.

Strains	MIC (µg/mL)		MBC (µg/mL)	
	AgOAc	Ag-NP	AgOAc	Ag-NP
P. aeruginosa				
PAO1	8	4	16	16
PAM57-15	8	4	16	16
PAHP3	8	4	16	16
S. aureus				
TCH1516	32	16	>256	>256
SALL06	32	16	>256	>256
SAEH05	16	8	64	16
Burkholderia sp.				
BG80	8	4	8	8
BM54	8	4	16	8

In summary, we have developed novel biocompatible and degradable polyphosphoester-based polymeric nanoparticles, which are capable of carrying silver cations *via* formation of silver acetylides with different coordination geometries, towards the treatment of lung infections associated with cystic fibrosis. The amphiphilic block terpolymer PEBP-*b*-PBYP-*g*-PEG was synthesized by "click-type" reactions, which are rapid, reliable and scalable. The amount of silver loaded into the micelles was quantified by inductively coupled plasma-mass spectrometry (ICP-MS) using rhodium as an internal standard. It was found that up to 15% (w/w) loading could be achieved, consuming most of the pendant alkyne groups along the backbone. Raman spectroscopy of Ag-loaded micelles revealed that silver was loaded into the nanoparticles mainly by two coordination geometries at a molar feed ratio of 1:1 (alkyne : silver acetate). A combination of DLS, TEM and AFM indicated that the nanoscopic polymer assemblies were well-defined, having a hydrodynamic diameter of *ca*. 11 nm, and that they underwent significant flattening upon adsorption onto substrates. The co-localization of silver, oxygen and phosphorous, visualized by EDS elemental mapping, further confirmed that silver was loaded into the polymeric matrices. It was found that silver was released in a sustained and controlled manner over 5 days, with release half-life values of 28 h in nanopure water and 16 h in 10 mM phosphate buffer containing 10 mM NaCl. The superior stability of silver cations when loaded into the micelles has the potential to avoid the inactivation by anions and other biological compounds in the human body. Furthermore, these silver-loaded nanoparticles were measured to have higher antimicrobial activities with much lower MICs and similar MBCs against a series of cystic fibrosis pathogens and lower toxicities to human bronchial epithelial cells *in vitro*, as compared to the free drug (silver acetate), demonstrating advantageous features of this nanoscopic silver delivery platform. Evaluation of these silver-loaded nanoparticles as antimicrobial agents for lung infections *in vivo*, as well as determination of their *in vitro* and *in vivo* degradation profiles, are currently under investigation.

Acknowledgements

Notes and references

aDepartment of Chemistry, Department of Chemical Engineering, and Department of Materials Science & Engineering, Laboratory for Synthetic-Biologic Interactions, Texas A&M University, P.O. Box 30012, 3255 TAMU, College Station, Texas 77842-3012, United States, Fax: +1 979 862 1137;Tel.: +1 979 845 4077; E-mail: wooley@chem.tamu.edu
bDepartment of Microbial Pathogenesis and Immunology, College of Medicine, Texas A&M Health Science Center, 407 Reynolds Medical Building, College Station, TX 77843-1114, United States, E-mail: cannon@medicine.tamhsc.edu

† Electronic Supplementary Information (ESI) available: Materials, experimental details, and characterization.. See DOI: 10.1039/b000000x/

1. L. Rizzello and P. P. Pompa, *Chem. Soc. Rev.*, 2014, **43**, 1501-1518.
2. H. W. Boucher, G. H. Talbot, J. S. Bradley, J. E. Edwards, D. Gilbert, L. B. Rice, M. Scheld, B. Spellberg and J. Bartlett, *Clin. Infect. Dis.*, 2009, **48**, 1-12.
3. *World Health Organization, World Health Statistics*, 2014, 45.
4. L. B. Rice, *J. Infect. Dis.*, 2008, **197**, 1079-1081.
5. G. W. Lau, H. M. Ran, F. S. Kong, D. J. Hassett and D. Mavrodi, *Infect. Immun.*, 2004, **72**, 4275-4278.
6. R. Laxminarayan, A. Duse, C. Wattal, A. K. M. Zaidi, H. F. L. Wertheim, N. Sumpradit, E. Vlieghe, G. L. Hara, I. M. Gould, H. Goossens, C. Greko, A. D. So, M. Bigdeli, G. Tomson, W. Woodhouse, E. Ombaka, A. Q. Peralta, F. N. Qamar, F. Mir, S. Kariuki, Z. A. Bhutta, A. Coates, R. Bergstrom, G. D. Wright, E. D. Brown and O. Cars, *Lancet Infect. Dis.*, 2013, **13**, 1057-1098.
7. T. Roemer and C. Boone, *Nat. Chem. Biol.*, 2013, **9**, 222-231.
8. J. Weers, *Adv. Drug. Deliv. Rev.*, 2014, in press, DOI: 10.1016/j.addr.2014.1008.1013.
9. H. J. Klasen, *Burns*, 2000, **26**, 131-138.
10. A. Gupta, K. Matsui, J. F. Lo and S. Silver, *Nat. Med.*, 1999, **5**, 183-188.
11. C. N. Lok, C. M. Ho, R. Chen, Q. Y. He, W. Y. Yu, H. Sun, P. K. Tam, J. F. Chiu and C. M. Che, *J. Biol. Inorg. Chem.*, 2007, **12**, 527-534.
12. A. D. Russell and W. B. Hugo, *Prog. Med. Chem.*, 1994, **31**, 351-370.
13. A. B. Lansdown, B. Sampson, P. Laupattarakasem and A. Vuttivirojana, *Br. J. Dermatol.*, 1997, **137**, 728-735.
14. S. L. Percival, P. G. Bowler and D. Russell, *J. Hosp. Infect.*, 2005, **60**, 1-7.
15. E. Hidalgo and C. Dominguez, *Toxicol. Lett.*, 1998, **98**, 169-179.
16. S. Silver, *FEMS Microbiol. Rev.*, 2003, **27**, 341-353.
17. C. L. Fox, Jr., *Arch. Surg.*, 1968, **96**, 184-188.
18. C. Ornelas-Megiatto, P. N. Shah, P. R. Wich, J. L. Cohen, J. A. Tagaev, J. A. Smolen, B. D. Wright, M. J. Panzner, W. J. Youngs, J. M. Frechet and C. L. Cannon, *Mol. Pharm.*, 2012, **9**, 3012-3022.
19. W. J. Youngs, A. R. Knapp, P. O. Wagers and C. A. Tessier, *Dalton Trans.*, 2012, **41**, 327-336.
20. Y. L. Li, K. Hindi, K. M. Watts, J. B. Taylor, K. Zhang, Z. C. Li, D. A. Hunstad, C. L. Cannon, W. J. Youngs and K. L. Wooley, *Chem. Commun.*, 2010, **46**, 121-123.
21. P. N. Shah, L. Y. Lin, J. A. Smolen, J. A. Tagaev, S. P. Gunsten, D. S. Han, G. S. Heo, Y. L. Li, F. W. Zhang, S. Y. Zhang, B. D. Wright, M. J. Panzner, W. J. Youngs, S. L. Brody, K. L. Wooley and C. L. Cannon, *ACS Nano*, 2013, **7**, 4977-4987.
22. E. A. Azzopardi, E. L. Ferguson and D. W. Thomas, *J. Antimicrob. Chemother.*, 2013, **68**, 257-274.
23. S. Y. Zhang, J. Zou, F. W. Zhang, M. Elsabahy, S. E. Felder, J. H. Zhu, D. J. Pochan and K. L. Wooley, *J. Am. Chem. Soc.*, 2012, **134**, 18467-18474.
24. M. Elsabahy, S. Zhang, F. Zhang, Z. J. Deng, Y. H. Lim, H. Wang, P. Parsamian, P. T. Hammond and K. L. Wooley, *Sci Rep*, 2013, **3**, 3313.
25. Y. F. Zhou, W. Huang, J. Y. Liu, X. Y. Zhu and D. Y. Yan, *Adv. Mater.*, 2010, **22**, 4567-4590.
26. Y. F. Shen, S. Y. Zhang, F. W. Zhang, A. Loftis, A. Pavia-Sanders, J. Zou, J. W. Fan, J. S. A. Taylor and K. L. Wooley, *Adv. Mater.*, 2013, **25**, 5609-+.
27. Z. Zhao, J. Wang, H. Q. Mao and K. W. Leong, *Adv. Drug Delivery Rev.*, 2003, **55**, 483-499.
28. U. Halbes-Letinois, J. M. Weibel and P. Pale, *Chem. Soc. Rev.*, 2007, **36**, 759-769.
29. Y. J. Su, M. Lu, B. L. Dong, H. Chen and X. D. Shi, *Adv. Synth. Catal.*, 2014, **356**, 692-696.
30. D. C. Kennedy, C. S. Mckay, L. L. Tay, Y. Rouleau and J. P. Pezacki, *Chem. Commun.*, 2011, **47**, 3156-3158.
31. X. Y. Meng, P. Q. Liao, J. Q. Liu and X. H. Bi, *Chem. Commun.*, 2014, **50**, 11837-11839.
32. A. Vila, H. Gill, O. McCallion and M. J. Alonso, *J. Control. Release*, 2004, **98**, 231-244.
33. A. Li, H. P. Luehmann, G. R. Sun, S. Samarajeewa, J. Zou, S. Y. Zhang, F. W. Zhang, M. J. Welch, Y. J. Liu and K. L. Wooley, *ACS Nano*, 2012, **6**, 8970-8982.
34. J. S. Suk, S. K. Lai, Y. Y. Wang, L. M. Ensign, P. L. Zeitlin, M. P. Boyle and J. Hanes, *Biomaterials*, 2009, **30**, 2591-2597.
35. B. C. Tang, M. Dawson, S. K. Lai, Y. Y. Wang, J. S. Suk, M. Yang, P. Zeitlin, M. P. Boyle, J. Fu and J. Hanes, *Proc. Natl. Acad. Sci. U. S. A.*, 2009, **106**, 19268-19273.
36. Y. Y. Wang, S. K. Lai, J. S. Suk, A. Pace, R. Cone and J. Hanes, *Angew. Chem. Int. Edit.*, 2008, **47**, 9726-9729.
37. F. W. Zhang, M. Elsabahy, S. Y. Zhang, L. Y. Lin, J. Zou and K. L. Wooley, *Nanoscale*, 2013, **5**, 3220-3225.
38. V. T. Huynh, G. J. Chen, P. de Souza and M. H. Stenzel, *Biomacromolecules*, 2011, **12**, 1738-1751.
39. C. E. Hoyle, A. B. Lowe and C. N. Bowman, *Chem. Soc. Rev.*, 2010, **39**, 1355-1387.
40. F. Cataido, *J. Raman Spectrosc.*, 2008, **39**, 169-176.
41. H. Feilchenfeld and M. J. Weaver, *J. Phys. Chem.*, 1989, **93**, 4276-4282.
42. A. Kumar, A. K. Pandey, S. S. Singh, R. Shanker and A. Dhawan, *Chemosphere*, 2011, **83**, 1124-1132.